

# A Highly Sensitive Temperature Sensor Based on a Liquid-Sealed S-Tapered Fiber

Rui Yang, Yong-Sen Yu, Yang Xue, Chao Chen, Chuang Wang, Feng Zhu, Bao-Lin Zhang, Qi-Dai Chen, and Hong-Bo Sun, *Member, IEEE*

**Abstract**—A highly sensitive temperature sensor based on the liquid-sealed S fiber taper (SFT) in a capillary is proposed and experimentally demonstrated. The temperature independent SFT is turned into a sensitive temperature sensor by the thermo-optic effect of the RI liquid and the thermal expansion of the sealant. The total length of the device is 10 mm, which can be further shortened to 1 mm if necessary. The temperature sensing mechanism of the liquid-sealed SFT is analyzed in detail and experimental results show the sensitivity reaches as high as  $-1.403 \text{ nm}/^\circ\text{C}$ . The temperature sensitivity contributions from different mechanisms are also obtained experimentally.

**Index Terms**—Fiber optic sensors, fiber tapers, temperature sensors.

## I. INTRODUCTION

**O**PTICAL fiber temperature sensors have many advantages, such as small size, fast response, corrosion resistance, and immunity to electromagnetic interference. They have been developed using various techniques, including fiber Bragg gratings (FBGs) [1], long period fiber gratings (LPFGs) [2], fiber interferometers [3] and other interesting structures [4], [5]. The FBGs are suitable for distributed temperature sensing and they have high detection accuracy, but the temperature sensitivity is usually low. To enhance the temperature sensitivity, the FBGs have been packaged in polymers, such as epoxy resin [6] and poly-dimethylsiloxane (PDMS) [7], or attached to metal slice [8] because the polymers and metal slice generally have high coefficients of thermal expansion (CTE). A phase shifted FBG has an even higher sensitivity to strain, and hence can be used for high sensitivity temperature sensing by attaching it to a high CTE material. The LPFGs also have been demonstrated with high temperature sensitivities [2], but they have strong cross sensitivities to refractive index (RI) and bending. Furthermore, these fiber-grating-based (FBGs and LPFGs) temperature sensors generally require precise and expensive fabrication techniques, including phase mask and laser source. The fiber interferometer temperature sensor has a

simple and easy fabrication process, but the sensitivity is still not satisfyingly high. The miniaturized fiber in-line temperature sensor [5] is high-temperature stable but its fabrication process is complicated, involving femtosecond laser micromachining [9]. Moreover, the temperature measurement around room temperature (RT) is significant, especially in the biological sensing field, because most of the living beings reveal the biological activity in this temperature range. Generally, organisms are sensitive to temperature, so the highly sensitive fiber temperature sensors are required in biological sensing, for example, the real-time temperature monitoring in organisms or cell culture solutions. However, most of the conventional fiber temperature sensors have a relatively low sensitivity due to the optical fibers made from silica material with low thermo-optic and thermal expansion coefficients. In order to enhance the temperature sensitivity, liquid sealing method is adopted in recent years' research [10]–[12]. The photonic crystal fibers (PCFs) are always used in these temperature sensors. Liquids with high thermo-optic coefficient are infiltrated into the microholes of a section of the PCF, which is then fusion spliced with single-mode fibers (SMFs) at both ends. By this means, fiber temperature sensors based on the fiber loop mirrors (FLMs) [10] and Mach-Zehnder interferometers (MZIs) [11], [12] are obtained. Their temperature sensitivities achieve as high as  $6.6 \text{ nm}/^\circ\text{C}$  [10] and  $-0.166 \text{ nm}/^\circ\text{C}$  [11], respectively. However, the FLM is still too long with the structure length of 6.1 cm, which is limited for integrated applications. The fiber MZI temperature sensor has a relatively low sensitivity and is not suitable for sensing in liquids because of the RI cross-sensitivity.

In this letter, we demonstrate a temperature sensor based on the S fiber taper (SFT) liquid-sealed in a capillary. The SFT is fabricated by applying off-axis pull while tapering the SMF in a fusion splicer [13]. It is insensitive to temperature, which has been demonstrated in [14], but highly sensitive to RI and axial tension. When the SFT is sealed in a capillary filled with RI liquid, its transmission spectrum will shift with temperature change. Because the RI value of the liquid and the tension in the sealant are temperature dependent, the RI around SFT and the axial tension in the taper will change with temperature, resulting in a sensitive temperature sensor. The sealed liquid is glycerin water solution with RI value of 1.4234, making the SFT highly sensitive to RI change. The sealant is AB glue, which has a relatively large thermal expansion coefficient. The temperature sensor has a total length of 1 cm, which is one-sixth of the alcohol-filled FLM [10] and can be much

Manuscript received January 31, 2013; revised March 4, 2013; accepted March 7, 2013. Date of publication March 12, 2013; date of current version April 10, 2013. This work was supported by the National Natural Science Foundation of China under Grants 90923037, 91123027 and 61137001.

The authors are with the State Key Laboratory on Integrated Optoelectronics, College of Electronic Science and Engineering, Jilin University, Changchun 130012, China (e-mail: yuys@jlu.edu.cn; chenqd@jlu.edu.cn).

Color versions of one or more of the figures in this letter are available online at <http://ieeexplore.ieee.org>.

Digital Object Identifier 10.1109/LPT.2013.2252336

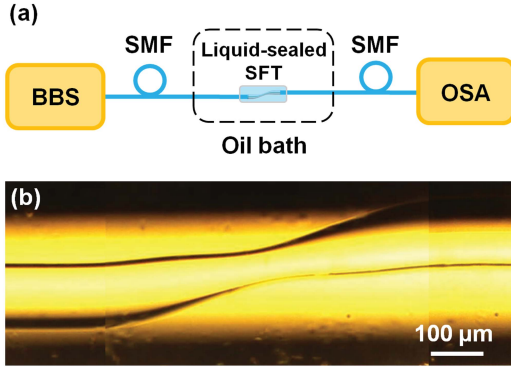


Fig. 1. (a) Experimental setup for the temperature sensing. (b) Optical microscope image of the liquid-sealed SFT in a glass capillary.

shorter if necessary. Its temperature sensitivity reaches  $-1.403 \text{ nm}/^\circ\text{C}$ , which is over 8 times higher than that of the isopropanol-sealed PCF in-line interferometer [11]. This novel temperature sensor has a simple fabrication process, compact size, and high sensitivity, making it a promising temperature sensor applied in biological sensing field.

## II. FABRICATION

The experimental setup for temperature sensing is illustrated in Fig. 1(a). The light from a supercontinuum broadband source (BBS) (Superk Compact, NKT Photonics, Inc.) propagates through the liquid-sealed SFT, and the transmission interference spectrum is measured by an optical spectrum analyzer (OSA) (Yokogawa AQ6370B) with a resolution of 0.1 nm. The SFT was fabricated on a standard telecom SMF (SMF-28e, Corning, Inc.) by using a fusion splicer (Ericsson FSU-975). Its detailed fabrication process was described in [14]. In our experiment, the discharge current, tapering time and fiber holders' axial offset were set as 10 mA, 10 s and 150  $\mu\text{m}$ , respectively. We obtained the SFT with geometrical parameters of 737  $\mu\text{m}$  in length, 62  $\mu\text{m}$  in waist diameter, and 125  $\mu\text{m}$  in axial offset, respectively. The SFT can be considered as a compact fiber MZI structure, which consists of two bending sections on both sides and one taper in the middle [Fig. 1(b)]. The fiber bending sections play the role of coupling light from core to the cladding or the reverse, and the fiber taper will enhance the measurement sensitivity [13]. Its transmission spectrum is shown in Fig. 2 (unsealed). Then, the SFT was inserted into a 1 cm-long glass capillary with an inner diameter of 300  $\mu\text{m}$ . A drop of the glycerin water solution with RI value of 1.4234 was added to one end of the capillary. Seconds later, the capillary tube was filled with the RI liquid via capillarity. In the end, we sealed two ends of the capillary with AB glue and obtained the temperature sensor. The optical microscope image of the SFT liquid-sealed in the capillary is shown in Fig. 1(b). The sensor length can be shortened to even 1 mm due to the SFT just having a length of hundreds of microns. After liquid sealing, the transmission spectrum of the SFT had a remarkable redshift, which is shown in Fig. 2 (liquid-sealed). The resonant dips of A, B, and C have the wavelength shift of 88.4 nm, 77.9 nm,

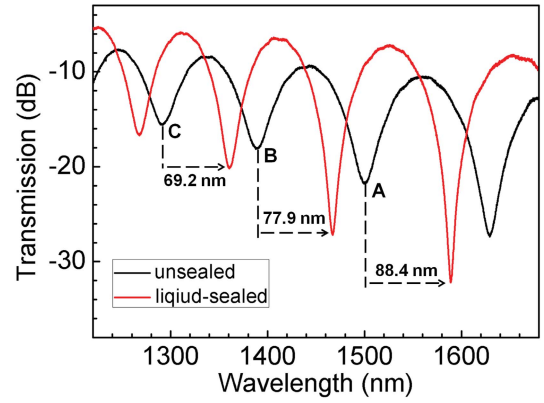


Fig. 2. Transmission spectra of the SFT before and after liquid sealing.

and 69.2 nm, respectively, indicating that the resonant dip at longer wavelength is higher sensitive to RI due to the cladding mode extending more evanescent field to environment at long wavelength.

## III. SENSING MECHANISMS

The SFT is temperature independent but highly sensitive to surrounding RI (SRI) and axial tension. With temperature augment, the RI value of the sealed liquid decreases by the negative thermo-optic coefficient. Meanwhile, the axial tension in the SFT is increasing, resulting from the thermal expansion of AB glue. In addition, the volume expansion of the liquid will produce hydraulic pressure on the glue, further increasing the axial tension. As we know, the transmission spectrum of the SFT has a blueshift when the SRI decreases or the axial tension increases. So the accumulation of the effects of RI liquid and AB glue will enhance the sensor's temperature sensitivity, which can be expressed as

$$S_T = S_T^{TO} + S_T^{TE} + S_T^{HP} \quad (1)$$

where  $S_T$  is the total temperature sensitivity of the liquid-sealed SFT,  $S_T^{TO}$  is the temperature sensitivity contribution (TSC) from thermo-optic effect of the RI liquid,  $S_T^{TE}$  is the TSC from thermal expansion effect of the AB glue, and  $S_T^{HP}$  is the TSC from hydraulic pressure of the liquid volume expansion. Here  $S_T^{TO}$  can be expressed as

$$S_T^{TO} = S_{RI} \times \gamma_{TO} \quad (2)$$

where  $S_{RI}$  is the RI sensitivity of the SFT,  $\gamma_{TO}$  is the thermo-optic coefficient of the RI liquid. In the RI measurement range, the sensitivity of the SFT increases with SRI augment, so we can choose the 1.4234-RI liquid, corresponding to the maximum  $S_{RI}$ , to enhance  $S_T^{TO}$ . The used RI liquid is made of glycerin water solution with volume ratio of 6 : 4. The thermo-optic coefficients of glycerin and water are  $-2.15 \times 10^{-4}/^\circ\text{C}$  and  $-1.45 \times 10^{-4}/^\circ\text{C}$ , respectively. We will use their weighted arithmetic average ( $-1.87 \times 10^{-4}/^\circ\text{C}$  for analysis later).

## IV. SENSING CHARACTERISTICS

The liquid-sealed SFT was immersed into an oil bath to test its temperature response. The oil bath has a temperature resolution of 0.01  $^\circ\text{C}$ . It was heated up from 20  $^\circ\text{C}$  to 50  $^\circ\text{C}$

in steps of 2.5 °C. The transmission spectrum of the liquid-sealed SFT has an obvious blueshift, as shown in Fig. 3(a). The resonant dips A, B, and C move to short wavelength with shifts of 40.8 nm, 35.2 nm, and 31.3 nm, respectively, when the temperature change is 30 °C. The transmission of each dip changes irregularly with temperature, which may be caused by the different influences from the variations of SRI and axial tension. According to our previous work [14], the transmission of each dip drops with the SRI decreasing and increases with the axial tension augments. For the liquid-sealed SFT, the irregular change of transmission dips with temperature is the result of the combined effects of RI and axial tension. The relationships between temperature and wavelength shift of these resonant dips are shown in Fig. 3(b). Their linear fitting results give the temperature sensitivities of about  $-1.403 \text{ nm}/^\circ\text{C}$ ,  $-1.212 \text{ nm}/^\circ\text{C}$ , and  $-1.094 \text{ nm}/^\circ\text{C}$ , respectively. The scatters of the points represent “errors” relative to the linear fittings. The errors of the presented device are relatively large due to the broad resonance bandwidth and instability of light source, leading to the difficulty in pinpointing the exact locations of the dips. In spite of the errors would not be thoroughly eliminated, they may be reduced by using some effective ways, such as adopting a more stable light source or appropriate filtering algorithm to improve the signal to noise ratio (SNR) and averaging the measurement results of two or more dips. In addition, because of the broad resonance bandwidth and high sensitivity, the proposed sensor could be demodulated through a cost effective OSA with a low resolution, e.g. 0.1 nm, reducing the overall cost of the system.

Although the temperature sensitivity of the liquid-sealed SFT depends on the S-taper exact shape and also on the packaging method, the sensor’s fabrication process is reproducible. If the fabrication conditions and sealing process are controlled precisely, ensuring the same S-taper shape and also the packaging strength, it is possible to obtain two reasonably identical sensors, which have the similar transmission spectra and temperature sensitivities. The reproducibility could be further improved through optimizing the fabrication process in the actual production. Besides, the resonance location in the transmission spectrum of the SFT also can be controlled by adjusting the fabrication parameters, such as the discharge current, tapering time and fiber holders’ axial offset. So a suitable resonance will appear in the required location if the appropriate fabrication parameters are chosen.

Compared to the FBG-based temperature sensors, the resonances of the SFT used are relatively broad with the 3 dB bandwidth or FWHM on the order of 10 nm, so the high sensitivity is obtained at the expense of this broadening of the resonances. The now accepted figure of merit for resonance-based sensor is proportional to the ratio of the sensitivity divided by the FWHM of the resonance [15]. So the sensor presented here has a sensitivity that is larger by 100 times over FBGs, but a width that is about 100 times worse. Therefore by that measure, the presented device has a similar figure of merit with FBGs to measure small temperature changes.

Moreover, we investigated the TSCs of  $S_T^{TO}$  and  $S_T^{TE}$  experimentally. The SFT was released and taken out of the capillary after the AB glue was dissolved by acetone. The

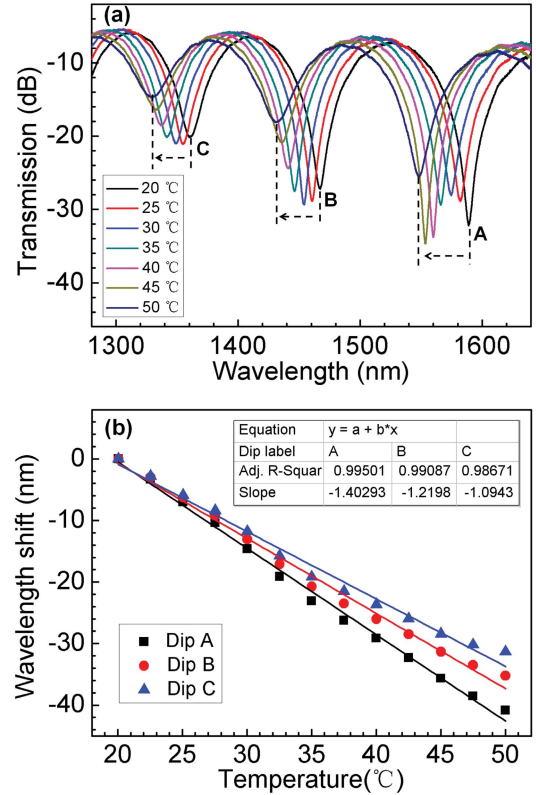


Fig. 3. (a) Transmission spectra of the liquid-sealed SFT under different temperatures. (b) Relationships between temperature and wavelength shift of the resonant dips.

RI measurement process was described in [14]. We obtained the relationships between SRI and wavelength shift of the resonant dips for the unsealed SFT, as shown in Fig. 4(a). The maximum RI sensitivities of the dips A, B and C are 3691 nm/RIU unit (RIU), 3137 nm/RIU, and 2794 nm/RIU, respectively, in the RI range of 1.4164~1.4234. As the thermo-optic coefficient of 1.4234-RI liquid is  $-1.87 \times 10^{-4}/^\circ\text{C}$ ,  $S_T^{TO}$  of the dips are calculated to  $-0.690 \text{ nm}/^\circ\text{C}$ ,  $-0.587 \text{ nm}/^\circ\text{C}$ , and  $-0.522 \text{ nm}/^\circ\text{C}$ , respectively. Later, the SFT was sealed again with AB glue, but this time only air was in the capillary. The temperature measurement of the air-sealed SFT was carried out in the oil bath. Thermal expansion effect of the AB glue made the resonant dips shifting to short wavelength. The relationships between temperature and wavelength shift of the resonant dips are shown in Fig. 4(b). The linear fitting results give the  $S_T^{TE}$  of the dips, which are  $-0.320 \text{ nm}/^\circ\text{C}$ ,  $-0.282 \text{ nm}/^\circ\text{C}$ , and  $-0.256 \text{ nm}/^\circ\text{C}$ , respectively. Take the dip A for example, its TSCs of  $S_T^{TO}$  and  $S_T^{TE}$  are  $-0.690 \text{ nm}/^\circ\text{C}$  and  $-0.320 \text{ nm}/^\circ\text{C}$ . The summation is  $-1.01 \text{ nm}/^\circ\text{C}$ , less than the temperature sensitivity of  $-1.403 \text{ nm}/^\circ\text{C}$ , corresponding to the liquid-sealed SFT. The difference value of  $-0.393 \text{ nm}/^\circ\text{C}$  is caused by the hydraulic pressure from the RI liquid volume expansion. It should be noted that the thermo-optic coefficient used in our theoretical expectation is that for unconstrained liquid. In the packaged device, the liquid is not free to expand and thus the change of RI with temperature cannot be the same as that of the same liquid in a volume that is free to expand.

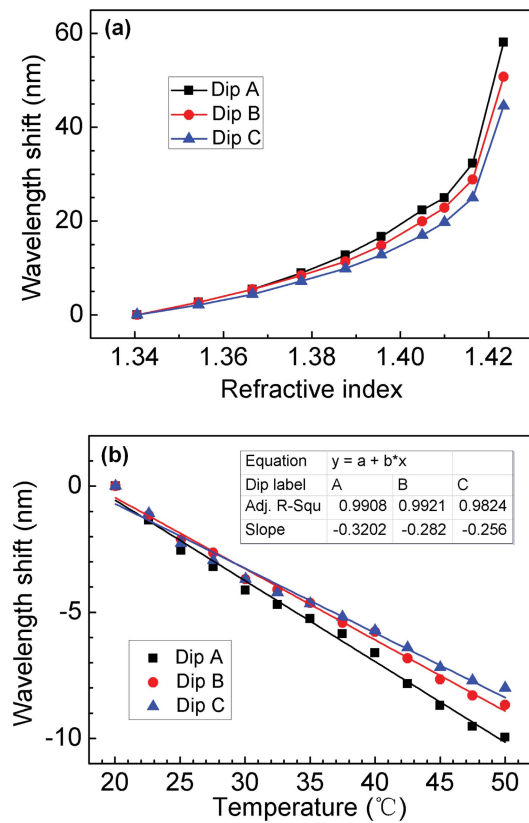


Fig. 4. (a) Relationships between SRI and wavelength shift of the resonant dips for the unsealed SFT. (b) Relationships between temperature and wavelength shift of the resonant dips for the air-sealed SFT.

The negative thermo-optic coefficient of the liquid may arise with temperature in the sealed capillary. So the TSC from thermo-optic effect of the RI liquid is overestimated and the TSC from hydraulic pressure could be much larger. Higher sensitivity can be acquired if we select the Cargille RI liquid, which has a thermo-optic coefficient of about  $-4 \times 10^{-4}/^{\circ}\text{C}$ , or some sealant having a higher thermal expansion coefficient.

## V. CONCLUSION

In conclusion, we fabricated a temperature sensor based on the SFT, which is liquid-sealed in a capillary. The thermo-optic effect of the RI liquid and the thermal expansion of the AB glue and sealed liquid turn the temperature independent SFT into a sensitive temperature sensor with the maximum sensitivity of  $-1.403 \text{ nm}/^{\circ}\text{C}$ . The sensing mechanism of the device has been analyzed in detail. In addition to the temperature test of the liquid-sealed SFT, experiments for the

SRI sensing of the unsealed SFT and temperature response of the air-sealed SFT are also carried out to get the TSCs from thermo-optic effect of the RI liquid and thermal expansion effect of the AB glue, respectively. The highly sensitive temperature sensor has the advantages of small size, ease of fabrication, and low cost, making it a good alternative fiber sensor in biological sensing field.

## REFERENCES

- [1] C. Chen, *et al.*, "Monitoring thermal effect in femtosecond laser interaction with glass by fiber Bragg grating," *J. Lightw. Technol.*, vol. 29, no. 14, pp. 2126–2130, Jul. 15, 2011.
- [2] X. Shu, L. Zhang, and I. Bennion, "Sensitivity characteristics of long-period fiber gratings," *J. Lightw. Technol.*, vol. 20, no. 2, pp. 255–266, Feb. 2002.
- [3] Y. Geng, X. Li, X. Tan, Y. Deng, and Y. Yu, "High-sensitivity Mach-Zehnder interferometric temperature fiber sensor based on a waist-enlarged fusion bitaper," *IEEE Sensors J.*, vol. 11, no. 11, pp. 2891–2894, Nov. 2011.
- [4] C. L. Lee, K. H. Lin, Y. Y. Lin, and J. M. Hsu, "Widely tunable and ultrasensitive leaky-guided multimode fiber interferometer based on refractive-index-matched coupling," *Opt. Lett.*, vol. 37, no. 3, pp. 302–304, Feb. 2012.
- [5] Y. Wang, Y. Li, C. Liao, D. N. Wang, M. Yang, and P. Lu, "High-temperature sensing using miniaturized fiber in-line Mach-Zehnder interferometer," *IEEE Photon. Technol. Lett.*, vol. 22, no. 1, pp. 39–41, Jan. 2010.
- [6] Q. Yu, Y. Zhang, Y. Dong, Y. P. Li, C. Wang, and H. Chen, "Study on optical fiber Bragg grating temperature sensors for human body temperature monitoring," in *Proc. Symp. Photon. Optoelectron.*, May 2012, pp. 1–4.
- [7] C. Park, K. Joo, S. W. Kang, and H. R. Kim, "A PDMS-coated optical fiber Bragg grating sensor for enhancing temperature sensitivity," *J. Opt. Soc. Korea*, vol. 15, no. 4, pp. 329–334, Dec. 2011.
- [8] Y. Li, W. Guo, and Y. Xie, "Temperature and strain characteristics of fiber Bragg grating packaged by brass slice," in *Proc. Int. Conf. Meas. Technol. Mech. Autom.*, vol. 3, Mar. 2010, pp. 734–737.
- [9] W. Xiong, Y. S. Zhou, X. N. He, Y. Gao, M. M. Samani, L. Jiang, T. Baldacchini, and Y. F. Lu, "Simultaneous additive and subtractive three-dimensional nanofabrication using integrated two-photon polymerization and multiphoton ablation," *Light, Sci. Appl.*, vol. 1, no. e6, Apr. 2012.
- [10] W. Qian, *et al.*, "High-sensitivity temperature sensor based on an alcohol-filled photonic crystal fiber loop mirror," *Opt. Lett.*, vol. 36, no. 9, pp. 1548–1550, May 2012.
- [11] S. Qiu, Y. Chen, F. Xu, and Y. Lu, "Temperature sensor based on an isopropanol-sealed photonic crystal fiber in-line interferometer with enhanced refractive index sensitivity," *Opt. Lett.*, vol. 37, no. 5, pp. 863–865, Mar. 2012.
- [12] W. Qian, *et al.*, "Temperature sensing based on ethanol-filled photonic crystal fiber modal interferometer," *IEEE Sensors J.*, vol. 12, no. 8, pp. 2593–2597, Aug. 2012.
- [13] R. Yang, Y. S. Yu, Y. Xue, C. Chen, Q. D. Chen, and H. B. Sun, "Single S-tapered fiber Mach-Zehnder interferometers," *Opt. Lett.*, vol. 36, no. 23, pp. 4482–4484, Dec. 2011.
- [14] R. Yang, *et al.*, "S-tapered fiber sensors for highly sensitive measurement of refractive index and axial strain," *J. Lightw. Technol.*, vol. 30, no. 19, pp. 3126–3132, Oct. 1, 2012.
- [15] I. M. White and X. Fan, "On the performance quantification of resonant refractive index sensors," *Opt. Express*, vol. 16, no. 2, pp. 1020–1028, Jan. 2008.